DMD Fast Forward. Published on September 13, 2010 as doi:10.1124/dmd.110.034793

20(S)-Ginsenoside Rh2 noncompetitively inhibits P-glycoprotein *in vitro* and *in vivo*: a case for herb-drug interactions

Jingwei Zhang, Fang Zhou, Xiaolan Wu, Yi Gu, Hua Ai, Yuanting Zheng, Yannan Li, Xiaoxuan Zhang, Gang Hao, Jianguo Sun, Ying Peng and Guangji Wang

Key Lab of Drug Metabolism and Pharmacokinetics, China Pharmaceutical University, Nanjing, Jiangsu, China (J.Z., F.Z., X.W., Y.G., H.A., Y.Z., Y.L., X.Z., G.H., J.S., Y.P., G.W.)

DMPK/Tox, Hutchison MediPharma Ltd., Shanghai, China (Y.G.)

Running title: 20(S)-Rh2 noncompetitively inhibits P-gp

Corresponding author: Prof. Guangji Wang, Ph.D., Key Lab of Drug Metabolism and Pharmacokinetics, China Pharmaceutical University, 24 Tong Jia Xiang, Nanjing, Jiangsu, 210009, P.R.China., E-mail: guangjiwang@hotmail.com, Tel: 86-25-83271128, Fax: 86-25-83271060

Number of text pages: 43

Number of tables: 2

Number of figures: 10

Number of references: 40

Number of words in the Abstract: 250

Number of words in the Introduction: 650

Number of words in the Discussion: 1409

ABBREVIATIONS

P-gp, P-glycoprotein; MDR, multi-drug resistance; FDA, Food and Drug Administration (USA); HBSS, Hank's balanced salt solution; Pi, inorganic phosphate; HPLC, High-performance liquid chromatography; FLD, fluorescence detector; LC-MS/MS, liquid chromatography tandem mass spectrometry; CMC-Na, carboxymethylcellulose; AUC, the area under the concentration-time curve; C_{max}, the maximum plasma concentration; $t_{1/2}$, half-life time; BSA, bovine serum albumin; TBS/T, Tris-buffered saline/Tween 20; S.E., standard error.

ABSTRACT

P-glycoprotein (P-gp) is an ATP-dependent efflux transporter highly expressed in gastrointestinal tract and multi-drug resistance tumor cells. Inhibition or induction of P-gp can cause drug-drug interactions and thus influence the effects of P-gp substrate drugs. Previous studies indicated that 20(S)-Rh2 could synergistically enhance the anti-cancer effects of conventional chemotherapeutic agents at a non-toxic dose. The aim of present study was to investigate *in vitro* and *in vivo* whether 20(S)-Rh2 was a P-gp inhibitor, and analyze the possible inhibitory mechanisms and potential herb-drug interactions. Results showed that *in vitro*, 20(S)-Rh2 significantly enhanced rhodamine 123 retention in cells, and decreased the efflux ratio of digoxin, fexofenadine and etoposide, which were comparable to the effects of the established P-gp inhibitor verapamil. However, the transport of 20(S)-Rh2 suggested 20(S)-Rh2 was not a P-gp substrate. Furthermore, the inhibitory effect persisted for at least 3 h after removal of 20(S)-Rh2. Unlike P-gp substrates, 20(S)-Rh2 inhibited both basal and verapamil-stimulated P-gp ATPase activities. It also significantly decreased UIC-2 binding fluorescence, a marker for conformational change of P-gp. *In situ* and *in vivo* experiments showed that 20(S)-Rh2 increased AUC and C_{max} of digoxin, fexofenadine and etoposide significantly without affecting terminal elimination half-time. Long-term treatment of 20(S)-Rh2 failed to affect intestinal P-gp expression *in vitro* and *in vivo*. In conclusion, 20(S)-Rh2 is a potent noncompetitive P-gp inhibitor, which indicates a potential herb-drug interaction when 20(S)-Rh2 is coadministered with P-gp substrate drugs. It could increase the absorption of P-gp

DMD Fast Forward. Published on September 13, 2010 as DOI: 10.1124/dmd.110.034793
This article has not been copyedited and formatted. The final version may differ from this version.

substrate drugs without a long-term induction of P-gp expression in rats.

INTRODUCTION

Traditional Chinese medicine (TCM) is an essential part of the healthcare system in several Asian countries for thousands of years (Qiu, 2007), and is also considered a complementary or alternative medical system in most Western countries. There is increasing evidence that TCM has been widely used in combination with chemical drugs. Hence, herb-drug interactions are now emerging and it has become necessary to investigate potential changes in drug efficacy and safety when herbs are coadministered (Chan et al., 2010). Pharmacokinetic herb-drug interactions related to metabolic enzymes have already attracted considerable attention (Rengelshausen et al., 2005). However, research on herb-drug interactions related to transporters is relatively limited, despite its important role in mediating drug disposition (Marchetti et al., 2007).

Ginsenosides are among the active ingredients of ginseng, the root of which has been used in traditional herbal remedies in Eastern Asia for over 2000 years and has recently attracted attention worldwide. 20(S)-Ginsenoside Rh2 (20(S)-Rh2), a trace constituent in ginseng, was first isolated from red ginseng by Kitagawa in 1983 (Kitagawa et al., 1983). It had a 20(S)-protopanaxadiol dammarane skeleton aglycone, and exhibited anti-cancer effects in various cancer cells *in vitro* (Fei et al., 2002; Kim et al., 2004). However, the anti-cancer activity of 20(S)-Rh2 was rather weak when compared to conventional chemotherapeutic agents. In addition, there are few reports on the anti-cancer effect of Rh2 itself *in vivo*. Though it is not ideal to use Rh2 singly as a chemotherapeutic agent, some synergetic effects between Rh2 and

chemotherapeutic agents have been reported from both *in vitro* and *in vivo* studies. Rh2 can reverse the resistance of daunomycin or vinblastine in P388/Adr cells (Hasegawa et al., 1995), synergistically enhance the activities of paclitaxel and mitoxantrone in prostate cancer cells (Jia et al., 2004; Xie et al., 2006) and increase the antitumor activity dose-dependently while decrease the genotoxic effects of cycolphosphamide (Wang et al., 2006). Most importantly, Rh2 enhanced the inhibitory effect of cisplatin on human ovarian cancer cells transplanted in nude mice at a non-effect dosage without any adverse effect (Kikuchi et al., 1991). A similar chemosensitizing effect towards paclitaxel was observed in nude mice bearing human prostate cancer LNCaP xenograft as well (Xie et al., 2006). However, despite these compelling findings, the synergistic mechanisms of 20(S)-Rh2 remain unclear, and most studies have focused on pharmacodynamic responses *in vitro*, such as cell cycle arrest and apoptosis. Of note though, Hasegawa *et al.* suspected that these synergistic effects might be related to a change in the activity of the efflux transporter P-glycoprotein (Hasegawa et al., 1995).

Our laboratory has focused on the pharmacokinetics of ginsenosides for a decade. In our previous studies, we found that the oral bioavailability of Rh2 was poor as a result of its low membrane permeability and the potential efflux mediated by ATP-binding cassette (ABC) transporters; it is mainly distributed in the intestine (Gu et al., 2006; Gu et al., 2009; Gu et al., 2010) where P-gp is highly expressed. In consideration of Hasegawa's hypothesis that Rh2 might interact with P-gp (Hasegawa et al., 1995), high levels of 20(S)-Rh2 in the intestine may result in some interactions

with some oral P-gp substrate drugs, such as etoposide (Nishimura et al., 2008) and paclitaxel (Bardelmeijer et al., 2000). The present study was designed to investigate whether 20(S)-Rh2 is a P-gp inhibitor and, if so, to elucidate its underlying inhibitory mechanism. We also sought to further analyze the potential pharmacokinetic-based herb-drug interactions related to drug transporters. In the process, it helped elucidate the synergetic effects of Rh2 with some chemotherapeutic agents as part of a long-term effort to identify efficient and safe P-gp modulators from natural products. This is an attractive contemporary strategy to promote the efficacy of anti-cancer drugs with adjunctive therapy or alternative medication, following successful examples of schisandrin B from Schisandra chinensis (Turcz.) Baill (Sun et al., 2007) and tetrandrine from Stephania tetrandra Moore (Fu et al., 2002).

MATERIALS AND METHODS

Animals

Male healthy Sprague–Dawley rats (180-250 g) were obtained from the Experimental Animal Breeding Center, Nanjing General Hospital of Nanjing Military Command (Nanjing, China) and were kept in room temperature (22 ± 1 ℃) , 50-60% relative humidity and automatic day-night rhythm (12 h-cycle). The animals were kept in these facilities for 1 week before the experiment. Prior to each experiment, the rats were fasted overnight (12 h) with free access to water. Animals were randomly assigned to different experimental groups. Animal experiments were carried out in accordance with the Guidelines for Animal Experimentation of China Pharmaceutical

University (Nanjing, China) and protocol was approved by the Animal Ethics Committee of this institution.

Materials

20(S)-ginsenoside Rh2 (purity > 98%) was purchased from Jilin University (Changchun, China). Rhodamine 123, digoxin, fexofenadine, etoposide, verapamil were purchased from Sigma Chemical Co. (St. Louis, MO). Digitoxin, loratadine were purchased from Chinese National Institute for the Control of Pharmaceutical and Biological Products (Beijing, China). [^{14}C] mannitol was purchased from Amersham Pharmacia Biotech (Buckinghamshire, UK). HPLC-grade acetonitrile and methanol were purchased from Sigma Chemical Co. (St. Louis, MO). Deionized water was prepared by Milli-Q system (Millipore, Milford, MA, USA) and was used throughout. Ethylacetate and all of other reagents, solvents were commercially available and of analytical grade.

Cell culture

Caco-2 cells (HTB-37) were obtained from American Type Culture Collection (Rockville, MD, USA). Cells were routinely cultured in DMEM supplemented with 10% fetal bovine serum, 1% nonessential amino acids, 1 mM sodium pyruvate, and 100 U/ml penicillin and streptomycin (Gibco-Invitrogen, USA). P-gp-overexpression MCF-7/Adr cells derived from parental MCF-7 cells by adriamycin selection were obtained from Institute of Hematology and Blood Diseases Hospital (Tianjin, China),

and cultured in RPMI 1640 supplemented with 10% fetal bovine serum, and 100 U/ml penicillin and streptomycin (Gibco-Invitrogen, USA).

The cells were grown in an atmosphere of 5% CO_2 at 37 ℃ and cell medium were changed every other day. Cells were passaged upon reaching ~80% confluence. All cells used in this study were between passage 30 to 38, and were negative for mycoplasma infection.

Cellular retention studies of rhodamine 123 by Caco-2 cells

The retention studies were performed with confluent epithelial monolayers of Caco-2 cells grown on 24-well plates. 20(S)-Rh2 and verapamil were prepared by dissolving in ethanol and dilution with HBSS. The final concentration of ethanol was 1% (v/v). Briefly, cultured cells were washed, and then preincubated in HBSS (37 ℃, pH 7.4) containing 20(S)-Rh2 (1, 5, 10 μM) or 1% ethanol (control) for 1.5 h, followed by the addition of 5 μM Rhodamine 123. Verapamil (10 μM) was used as a positive control inhibitor. After incubation for another 2 h, the retention was stopped by rinsing the cells with ice-cold HBSS for three times. Cells were lysed by three freeze-thaw cycles, and protein concentrations were measured by the method of Bradford. Rhodamine 123 concentration was determined by HPLC-FLD. All experiments were conducted in triplicate.

Inhibition of P-gp substrate transport by 20(S)-Rh2 in Caco-2 cell monolayers

Briefly, Caco-2 cells with a density of 1.2×10^5 cells/insert were seeded on a

permeable polycarbonate insert (Millicell cell culture inserts, 0.4-μm pore size, 12 mm diameter, Millipore, USA) in 24-well tissue culture plates, and were used for the experiment 18-21 days after seeding. [^{14}C] mannitol permeability and TEER measurements (Millicell-ERS epithelial Voltohmmeter, Millipore Co., Milford, MA) were used to evaluate the integrity of Caco-2 cell monolayers. The monolayers used in transport studies had TEER value exceeding 600 Ω·cm^2 and the leakage of mannitol was less than 0.3% of the dose/h.

On the day of an experiment, before initiation of transport studies, the cell monolayers were first washed with warm HBSS (pH 7.4) twice. HBSS containing 20(S)-Rh2 (1, 5, 10 μM) or 1% ethanol (control) was then loaded into both apical and basolateral chambers. After incubation at 37 ℃ for 1.5 h, 5 μM digoxin or 10 μM fexofenadine or 10 μM etoposide was added to either apical or basolateral side to evaluate the transport in absorptive and secretory direction respectively, and the cell monolayers were incubated for another 2 h. Verapamil (10 μM) was used as a positive control. At the designated time point, samples were taken from the receiving chamber for analysis. Digoxin, fexofenadine and etoposide levels were determined by LC-MS/MS. All experiments were conducted in triplicate.

Transport studies of 20(S)-Rh2 across Caco-2 cell monolayers

Caco-2 cells were cultured in the same manner as described before. HBSS containing 20(S)-Rh2 (1, 5, 10 μM) or digoxin (positive P-gp substrate) was loaded into either apical or basolateral chambers, in the absence or presence of 10 μM verapamil

(positive P-gp inhibitor). After incubation at 37 ℃ for 1.5 h, aliquots from the receiver compartment were collected for determination of 20(S)-Rh2 or digoxin. The concentration of 20(S)-Rh2 was quantitated by LC-MS as described previously (Gu et al., 2006).

Duration of P-gp inhibitory effect of 20(S)-Rh2

To evaluate the duration of action of 20(S)-Rh2 as a P-gp inhibitor, Caco-2 cells were incubated with 20(S)-Rh2 (10 μM) or verapamil (10 μM) for 1.5 h, then were washed to discard 20(S)-Rh2 or verapamil, and were incubated for the designated time (0, 30, 60, 180 min) in the absence of 20(S)-Rh2 or verapamil, prior to the addition of 5 μM rhodamine 123. The accumulation of rhodamine 123 lasted for 2 h. The intracellular concentration of rhodamine 123 was quantitated as described before. All experiments were conducted in triplicate.

P-gp ATPase activity assay

Human P-gp-overexpressing membranes obtained from baculovirus-infected insect cells (BD Biosciences, USA) were analyzed for both vanadate-sensitive basal and drug-stimulated ATP consumption, in the absence or presence of 20(S)-Rh2. The inorganic phosphate released from ATP was measured by colorimetric detection at 880 nm to evaluate the activity of P-gp ATPase. All steps in the procedure were based on the manufacturer's protocol (Human P-gp Membranes 5mg/ml, BD Gentest^{TM}, BD Bioscience, USA) with minor modification. Briefly, membranes (15 μg/well) prepared

in Tris/Mes buffer, pH 6.8 (50 mM Tris/4-morpholineethanesulfonic acid, pH 6.8, 50 mM KCl, 5 mM sodium azide, 2 mM EGTA, and 2 mM DL-dithiothreitol) were incubated at 37 ℃ on a 96-well plate for 5 min with 20(S)-Rh2 (0.5, 1, 5, 10, 20 μM) in the presence or absence of 100 μM sodium orthovanadate (in triplicate). Verapamil (20 μM) was used as a positive control. 12 mM Mg-ATP (20 μl) was added to initiate the reaction. The 60 μl reaction mixture was incubated at 37 ℃ for 60 min, and then was terminated by addition of 10% SDS containing antifoam A (30 μl). The inorganic phosphate released was detected by incubation at 37 ℃ for 20 min with 200 μl of detection reagent [1:4 v/v mixture of 35 mM ammonium molybdate in 15 mM zinc acetate (pH 5.0) and 10% ascorbic acid]. The drug-stimulated ATPase activity (nmol/min/mg protein) was determined as the difference between the amounts of inorganic phosphate released from ATP in the absence and presence of vanadate.

For the inhibition studies of 20(S)-Rh2, verapamil-stimulated activity was assayed in the presence of 20 μM verapamil plus or minus increasing concentrations of 20(S)-Rh2 (1, 5, 10 μM), using the method mentioned above.

MDR1 shift assay

The MDR1 shift assay was performed according to the manufacturer's protocol (MDR1 Shift Assay, Chemicon, Millipore, USA). Approximately 1×10^6 MCF-7/Adr cells suspended in UIC-2 binding buffer (1×PBS, 1% BSA) were pre-warmed in a water bath at 37 ℃ for 10 min, followed by incubation in the absence or presence of 20(S)-Rh2(1, 10 μM), 10 μM vinblastine (as P-gp competitive inhibitor), or 1 mM

sodium orthovanadate (as P-gp noncompetitive inhibitor) at 37 ℃ for another 15 min. Then 2.5 μg monoclonal antibody UIC2 was added. After incubation at 37 ℃ for another 15 min, 1 ml ice-cold UIC2 binding buffer was added to stop the reaction. The cells were washed twice and then 250 μl ice-cold Phycoerythrin-Labeled Anti-Mouse IgG was added. After 15 min at 4 ℃ in the dark, samples were washed and re-suspended in 0.5 ml ice-cold UIC2 binding buffer and further analyzed by flow cytometer (Beckman Coulter cytomics FC 500, USA).

***In situ* single-pass perfusion experiment in rats**

Briefly, rats were anesthetized with an intra-peritoneal phenobarbital sodium and placed on a heating surface to maintain a body temperature at 37 ℃. The abdomen was opened by a middle incision of 3-4 cm. An ileal segment of approximately 10 cm was isolated and cannulated on two ends with flexible plastic tubing. The ileal segment was flushed with normal saline to clean out any residual debris. Blank Kreb-Ringer's buffer (NaCl 128.5 mM, KCl 4.7 mM, $MgCl_2$ 2.3 mM, $CaCl_2$ 3.3 mM, $NaH_2PO_4 \cdot 2H_2O$ 1.87 mM, $NaHCO_3$ 16.3 mM, glucose 7.8 mM, and phenol red 20 μg/ml, adjusted to pH 6.8 with 1.0 M phosphoric acid, 37 ℃) was then pre-infused for 15 min by an infusion pump at a flow rate of 1.0 ml/min. After that, Kreb-Ringer's buffer containing 1 μM rhodamine 123 in the absence or presence of 20(S)-Rh2 (1, 5, 10 μM) was perfused at a flow rate of 0.2 ml/min through the intestinal segment.

Perfusate samples obtained from the outlet of ileum were collected every 20 min for 2 h. The radius and the length of the ileal segment were measured at the end

of the experiment. During the whole course, care was taken to avoid disturbance of the circulatory system, and the exposed segment was kept moist with 37 ℃ normal saline solution. Phenol red, the non-absorbable marker for measuring water flux and correcting for water changes across the incised ileal segment, was determined using a spectrophotometer.

***In vivo* pharmacokinetic studies**

To evaluate the effect of single dose of 20(S)-Rh2 on the pharmacokinetics of each P-gp substrate, rats were divided into 2 groups with five animals each. One received a single dose of 20(S)-Rh2 intragastrically at 25 mg/kg suspended in 0.5% CMC-Na, while the other received the vehicle (0.5% CMC-Na) serving as the control. Two hours later, a P-gp substrate, digoxin (0.25 mg/kg), fexofenadine (10 mg/kg) or etoposide (10 mg/kg) was given to the rats by intragastric administration.

To evaluate the effect of long-term treatment of 20(S)-Rh2 on the pharmacokinetics of etoposide, rats were also divided into 2 groups with five animals each. One received a dose of 20(S)-Rh2 intragastrically at 25 mg/kg suspended in 0.5% CMC-Na, once a day, for 10 successive days, while the other received the vehicle (0.5% CMC-Na) serving as the control. On the 11^{th} day, etoposide was administered intragastrically to rats with a single dose of 10 mg/kg.

In the both studies, blood samples were collected before the P-gp substrate dosing and at 5, 10, 15, 30, 45, 60, 120, 240, 360, 480 min post-digoxin-dosing or 5, 10, 20, 30, 45, 60, 120, 240, 420, 600 min post- fexofenadine-dosing or 5, 10, 15, 30,

45, 60, 90, 120, 240, 360, 480 min post-etoposide-dosing into heparinized tubes. Plasma was obtained by centrifugation at 5000 g for 10 min and stored at -20 □ before analysis.

Effects of 20(S)-Rh2 on the basal intestinal P-gp expression *in vitro* and *in vivo*

Caco-2 cells cultured routinely in 75 cm^2 flasks were exposed to 1 μM 20(S)-Rh2, 10 μM 20(S)-Rh2 or ethanol (1%, v/v) as vehicle control after reaching 70% confluence. After exposure for 24 h, 48 h, 72 h, the cells were harvested, and stored at -80 ℃ for western blotting analysis.

The rats receiving etoposide after long-term treatment with 20(S)-Rh2 were euthanized after blood collection. Ileal segment of the intestines were immediately excised, washed with normal saline and stored at -80℃ until Western blotting analysis.

Western Blotting Analysis

Cells or intestinal homogenates were lysed in ice-cold radioimmunoprecipitation assay (RIPA) lysis buffer with 0.02 mM phenylmethanesulfonyl fluoride (PMSF) for 30 min, and then ultrasonicated for 60 sec at intervals in ice-bathe. Samples were then centrifuged at 500 g for 10 min at 4 ℃. The supernatant was transferred to a new tube and centrifuged at 15000 g for 60 min at 4 ℃. The supernatant (cytosol protein, such as β-actin) and precipitation (membrane protein, such as P-gp) were both collected and stored at -80 ℃ until use. Protein concentrations were measured using a BCA

DMD Fast Forward. Published on September 13, 2010 as DOI: 10.1124/dmd.110.034793
This article has not been copyedited and formatted. The final version may differ from this version.

protein assay kit (Pierce Chemical, Rockford, IL, USA) according to the manufacturer's instructions. Samples reconstituted in SDS-PAGE sample loading buffer were boiled for 5 min for protein denaturation. Protein samples were separated on an 8% SDS-polyacrlyamide gel and transferred onto a PVDF membrane (Millipore, USA). After blotting, the membrane was blocked with 10% BSA in TBS/T for 1 h at 37 ℃. Immunoblots were incubated with the primary monoclonal antibody to P-gp (1:800, clone3C3.2, Millipore, USA) or β-actin (1:800, Bioworlde, USA) for 24 h at 4 ℃. The membrane was washed (4×10 min), incubated with secondary antibody horseradish peroxidase-conjugated goat anti-mouse IgG (1:800, Boster Biological Technology, China) for 1 h at 37 ℃ and then washed three times with TBS/T. The signals were detected using an enhanced chemiluminescence kit (Pierce Chemical, Rockford, IL, USA). The P-gp protein band intensity was normalized to that of β-actin.

Analytical Methodology

Analysis of rhodamine 123 in cell lysates and buffer samples

Briefly, an aliquot of 100 μl sample was protein-precipitated with 300 μl acetonitrile. After centrifugation, 20 μl of the supernatant was injected into a Shimadzu LC-10Avp system (Shimadzu, Japan) coupled with a fluorescence detector (RF-10A_{XL}) with the excitation wavelength set at 485 nm and emission wavelength 546 nm. The chromatographic conditions were as follows: column, Kromosil ODS (KR100-5C18, 250×4.6 mm, 5 μm) (Kka Chemicals AB, Sweden); mobile phase, 0.1% acetic acid/

DMD Fast Forward. Published on September 13, 2010 as DOI: 10.1124/dmd.110.034793
This article has not been copyedited and formatted. The final version may differ from this version.

acetonitrile = 65/35 (v/v); column temperature, 40 ℃; flow rate, 1 ml/min. Quantitation was based on the external standard method.

Analysis of digoxin, fexofenadine and etoposide in cell lysates, buffer samples and rat plasma

An aliquot of 100 μl sample with 10 μl of internal standard spiked was extracted by 1 ml ethylacetate. After centrifugation, 900 μl of the extracted organic layer was evaporated to dryness by Thermo Savant SPD 2010 SpeedVac System (Thermo Electron Corporation, USA). The residue was reconstituted in 100 μl acetonitrile, followed by another centrifugation. The 10 μl of the supernatant was injected for LC-MS/MS analysis. The system consisted of a Finnigan Surveyor^{TM} HPLC system (Thermo Electron, San Jose, CA, USA) and Finnigan TSQ Quantum Discovery Max system (Thermo Electron), equipped with an electrospray ionization source. Data acquisition was performed with Xcalibur 2.0 software (Thermo Finnigan). The analytical columns were a Gemini C18 column (150×2.0 mm, 3 μm, Phenomenex, USA) for analysis of digoxin and a Cosmosil ODS column (5C18-MS-II, 150×2.0 mm, 5 μm, Nacalai Tesque, Japan) for analysis of fexofenadine and etoposide. The column and autosampler tray temperatures were 40 and 4 ℃, respectively. Detailed LC conditions and mass parameters are shown in Table 1.

Data analysis

For the transport assay, the apparent permeability coefficient (P_{app}) is presented

in cm/sec, and calculated as following equation

$$P_{app} = \frac{\Delta Q}{\Delta t} \cdot \frac{1}{60} \cdot \frac{1}{A} \cdot \frac{1}{C_0} \qquad (1)$$

Where $\Delta Q / \Delta t$ is the permeability rate (nmol/sec); A is the surface area of the membrane (cm^2); and C_0 is the initial concentration in the donor chamber (nM). The efflux ratio (ER) was calculated as:

$$ER = \frac{P_{app}(BL - AP)}{P_{app}(AP - BL)} \qquad (2)$$

In single-pass perfusion assay, absorption rate constant k_a and $C_{out(corr)}$ were calculated from equation (3) and (4).

$$k_a = \left(1 - \frac{C_{out(corr)}}{C_{in}}\right) \times \frac{Q}{V} \qquad (3)$$

and

$$C_{out(corr)} = C_{out} \times \frac{C(PR)_{in}}{C(PR)_{out}} \qquad (4)$$

Drug permeability across rat ileum (P_{eff}) was calculated from Eq (5).

$$P_{eff} = -\frac{Q}{A} \cdot Ln(C_{out(corr)} / C_{in}) \qquad (5)$$

$C(PR)_{in}$ and $C(PR)_{out}$ are the inlet and outlet phenol red (PR) concentrations, respectively; $C_{out(corr)}$ is the water flux corrected outlet concentration of rhodamine 123 at specific time interval; C_{in} denotes the inlet rhodamine 123 concentration; Q is the flow rate through the ileal segment, while V and A are the volume and surface area of perfused segment respectively.

Pharmacokinetic parameters of P-gp substrates were obtained by noncompartmental analysis using DAS (Drug and Statistics, version 2.1, Chinese

Pharmacological Society). The area under the plasma concentration-time curve (AUC) was calculated using the trapezoidal method. The terminal half-life ($t_{1/2}$) was calculated as ln2/k, where k, the elimination rate constant, was determined from the slope of the terminal regression line.

Data are expressed as mean ± S.E.. Comparisons for between-groups were performed using Student's *t* test. For multiple comparisons, one-way analysis of variance (ANOVA) followed by Post-Hoc test was adopted. The difference was considered to be statistically significant if the probability value was less than 0.05 ($p<0.05$).

RESULTS

20(S)-Rh2 increased the cellular retention of rhodamine 123 by Caco-2 cells.

Intracellular accumulation of rhodamine 123, a classic P-gp fluorescence substrate for rapid screening, was tested to explore the inhibitory potential of 20(S)-Rh2 on P-gp. 20(S)-Rh2 concentration-dependently increased cellular retention of rhodamine 123 in Caco-2 cells by 1.26-, 1.92- and 2.53-fold in the presence of 1, 5, 10 μM 20(S)-Rh2, respectively ($p<0.01$) (Fig 2). The established P-gp inhibitor verapamil (10 μM) exhibited a potent inhibitory effect on P-gp, resulting in a significant 1.92-fold increase of intracellular accumulation of rhodamine 123 ($p<0.01$).

20(S)-Rh2 decreased the efflux ratio of digoxin, fexofenadine and etoposide across Caco-2 monolayers.

The flux of digoxin (5 μM), fexofenadine (10 μM) and etoposide (10 μM) across Caco-2 cell monolayers in the absorptive (AP-BL) and secretory (BL-AP) directions and the corresponding P_{app} values are shown in Fig 3. Digoxin, fexofenadine and etoposide exhibited highly polarized transport across Caco-2 cell monolayers with marked efflux ratios. The presence of 20(S)-Rh2 or verapamil (the positive control inhibitor) significantly and in a concentration-dependent manner decreased the transport of digoxin, fexofenadine or etoposide across Caco-2 monolayers in the BL-AP direction, but increased digoxin or etoposide transport in AP-BL direction, which correspondingly led to the decrease of efflux ratios.

20(S)-Rh2 exhibited no polarized transport mediated by P-gp across Caco-2 cell monolayers

The Papp values of 20(S)-Rh2 in both AP-BL and BL-AP directions at all concentrations were approximately 10^{-7} cm/sec, which indicated poor transmembrane permeability of 20(S)-Rh2. In addition, the efflux ratio of 20(S)-Rh2 was about 2.0, which is considered a threshold for defining whether a drug is a substrate of P-gp or not. Furthermore, the efflux ratio of 20(S)-Rh2 was not changed in the presence of 10 μM verapamil. In contrast, classic P-gp substrate digoxin possessed an efflux ratio of 6.6, which was far above 2.0. And this high efflux ratio of digoxin decreased to 1.3 significantly in the presence of 10 μM verapamil. Thus, 20(S)-Rh2 is not a substrate of P-gp.

20(S)-Rh2 inhibited P-gp function for at least 3 h after being removed

After incubating with Caco-2 cells for 1.5 h, 20(S)-Rh2 was removed from the cell culture. Throughout the following 0 to 180 min, the P-gp inhibitory effect was still present, as the intracellular accumulations of rhodamine 123 at various time point were nearly the same as that at T_0 (Fig 5). Conversely, the competitive P-gp inhibitor verapamil lost its effect rapidly as soon as it was removed, and the intracellular accumulation of rhodamine 123 was not more than half of that at T_0.

20(S)-Rh2 inhibited the basal and verapamil-stimulated P-gp ATPase activity

The efflux activity of P-gp is ATP dependent, and expression of P-gp results in the appearance of a vanadate-sensitive drug-stimulated ATPase activity. Fig 6A shows the basal and verapamil-stimulated P-gp ATPase activity, and also the effects of various concentrations of 20(S)-Rh2 on P-gp ATPase. Verapamil, a known substrate of P-gp, significantly stimulated ATPase activity at 20 μM. In contrast, 20(S)-Rh2 did not show stimulation at 0.5, 1 and 5 μM, but exhibited an inhibition at 10 and 20 μM (p<0.05). This result suggested that 20(S)-Rh2 may be an inhibitor, but not a substrate of P-gp (Chang et al., 2006).

The effect of 20(S)-Rh2 on verapamil-stimulated ATPase activity was also investigated. The production of inorganic phosphate stimulated by 20 μM verapamil in the absence or presence of 20(S)-Rh2 (1, 5, 10 μM) was measured. The data showed that 20(S)-Rh2 inhibited verapamil-stimulated P-gp ATPase significantly and in a concentration-dependent manner (Fig 6B). Moreover, 10 μM 20(S)-Rh2 reduced

the P-gp ATPase activity close to the basal level.

20(S)-Rh2 changes the binding of conformation-sensitive antibody to P-gp

UIC2, which reacts with an extracellular domain of P-gp, is a conformation-sensitive mouse monoclonal antibody against human MDR1. There is evidence that the presence of P-gp substrates and/or competitive inhibitors increase the reactivity of UIC2 drastically, while allosteric modulators that interfere with substrate binding indirectly reduced UIC2 reactivity (Mechetner et al., 1997; Maki et al., 2003). The results showed that the P-gp substrate and competitive inhibitor vinblastine at 10 μM increased UIC2 binding remarkably, while the allosteric inhibitor sodium orthovanadate decreased UIC2 binding significantly at 1 mM. As shown in Fig 7, 20(S)-Rh2 did not influence UIC2 binding at 1 μM, but caused a decrease at 10 μM, similar to sodium orthovanadate which inhibits P-gp function by trapping it as a P-gp-ADP-Vi complex.

20(S)-Rh2 increased rhodamine123 *in-situ* ileal permeability in the single-pass intestinal perfusion model in rats

To further explore whether the inhibitory effect of 20(S)-Rh2 on P-gp could result in herb-drug interactions with P-gp substrates in the intestinal tract, *in situ* single pass intestinal perfusion experiments with rat ileum was performed to calculate the absorption rate constant and intestinal permeability of rhodamine 123 in the presence or absence of various concentrations of 20(S)-Rh2. Steady state fluxes of

rhodamine123 in the presence of 20(S)-Rh2 (1, 5, 10 μM) are shown in Table 2. In the presence of 20(S)-Rh2, intestinal permeability and the absorption rate constant of rhodamine123 significantly increased in a concentration-dependent manner. These results clearly showed that 20(S)-Rh2 promoted the intestinal absorption of the classic P-gp substrate rhodamine123 by circumvention of P-gp mediated efflux.

Single dose 20(S)-Rh2 increased plasma concentrations of P-gp substrates in rats

To assess whether the *in vitro* P-gp inhibitory effect of 20(S)-Rh2 also occurred *in vivo*, the pharmacokinetics of three P-gp substrates, following intragastric administration, were determined in SD male rats with or without 20(S)-Rh2. Plasma concentration versus time curves of digoxin, fexofenadine or etoposide following intragastric administration in the absence and presence of 20(S)-Rh2 are depicted in Fig 8. As shown in Fig 8A, coadministration of 20(S)-Rh2 (25 mg/kg) significantly increased the AUC of digoxin 1.67-fold, from 929.6 ± 156.0 ng/ml·min in the vehicle-treated group to 1549.3 ± 158.6 ng/ml·min in the 20(S)-Rh2-treated group. C_{max} increased 1.51-fold, from 9.9 ± 1.2 ng/ml in the vehicle-treated group to 14.9 ± 1.6 ng/ml in the 20(S)-Rh2-treated group. The terminal $t_{1/2}$ was not significantly changed following 20(S)-Rh2 treatment.

Fexofenadine, the metabolite of terfenadine, had been reported as a P-gp substrate and its intestinal absorption is controlled in part by P-gp (Petri et al., 2004; Ujie et al., 2008). Administration of 20(S)-Rh2 (25 mg/kg) 2 h prior to fexofenadine in rats had significant effects on plasma pharmacokinetic parameters of fexofenadine

(Fig 8B). The AUC of fexofenadine in 20(S)-Rh2 pre-treated group was 39181.6 ± 8923.7 ng/ml·min, significantly higher than that in control group (16206.5 ± 1803.6 ng/ml·min) by 2.42-fold, and C_{max} increased by 3.46-fold (405.2 ± 128.2 ng/ml in 20(S)-Rh2 pre-treated group, 117.0 ± 32.1 ng/ml in control group). Other parameters were not significantly changed by 20(S)-Rh2.

Etoposide, a natural product used for the treatment of malignancies, had been widely used as P-gp substrate in experiments (Takeuchi et al., 2006; Xu et al., 2006). The plasma etoposide concentrations after a single dose of 25 mg/kg 20(S)-Rh2 were increased compared to those of control group (Fig 8C). The AUC of etoposide was increased by 4.52-fold after 20(S)-Rh2 treatment (111337.1 ± 28909.2 *vs* 503646.8 ± 109286.8 ng/ml·min). In addition, 20(S)-Rh2 increased the etoposide C_{max} value by 2.54-fold compared to that of control (1062.5 ± 202.9 *vs* 2693.9 ± 682.1 ng/ml). The terminal $t_{1/2}$ showed no difference between 20(S)-Rh2-treated and control groups.

Long-term treatment of 20(S)-Rh2 failed to affect the pharmacokinetics of etoposide in rats

As shown in Fig 9, no significant difference in the C_{max} (750.7 ± 91.8 *vs* 738.9 ± 78.2 ng/ml), AUC (84564.9 ± 8347.0 *vs* 80965.5 ± 6263.2 ng/ml·min) and terminal $t_{1/2}$ (107.8 ± 10.6 *vs* 103.4 ± 11.2 min) of etoposide was observed between the control group and 20(S)-Rh2-10-successive-day-treated group.

20(S)-Rh2 did not influence the basal P-gp expression *in vitro* and *in vivo*

To investigate the effects of 20(S)-Rh2 on basal P-gp expression *in vitro*, after Caco-2 cells were treated with 20(S)-Rh2 for 24 h, 48 h, 72 h respectively, the lysates were recovered and subjected to Western blot analysis. As shown in Fig 10A, compared with control cells which were not exposed to 20(S)-Rh2, the P-gp level in the 20(S)-Rh2 treated cells was not altered significantly.

In an analysis of ileum homogenate samples collected from the rats treated with 20(S)-Rh2 for 10 successive days in Fig 10B, there was no significant difference between the control group and 20(S)-Rh2 treated groups, which also indicated that 20(S)-Rh2 had no effect on basal intestinal P-gp expression *in vivo*.

DISCUSSION

P-gp, an extruding transporter, is highly expressed in gastrointestinal tract and can form a biological barrier against xenobitotic agents. Thus it can be a major determinant of drug pharmacokinetic behavior. Inhibition or induction of P-gp has been reported to be one of the causes of drug-drug interactions (DDI) in animals and humans. On one hand, DDI should be avoided as it might cause severe clinical side effects. On the other, a DDI sometimes might benefit the patients by producing an enhanced effect from increased systemic levels of the target drug. The synergistic effect of Rh2 on anticancer therapies has already been reported (Jia et al., 2004; Wang et al., 2006; Xie et al., 2006). In the present study, the pharmacokinetic-basis for this synergism was elucidated.

Caco-2 cell monolayers, which originate from a human colonic adenocarcinoma

cell line, not only have been used widely as a model for drug intestinal absorption studies, but also are often used as a model to analyze the possible DDIs involving P-gp, due to its rich P-gp expression in the apcial membrane. It was found that 20(S)-Rh2 markedly increased the intracellular fluorescence of P-gp substrate rhodamine 123, and inhibited the transport of three typical P-gp substrates (digoxin, fexofenadine and etoposide), confirming that 20(S)-Rh2 is a potent P-gp inhibitor, comparable to the established P-gp inhibitor, verapamil.

Recently 20(S)-protopanaxadiol, the metabolite of 20(S)-Rh2, was shown to inhibit P-gp in multidrug resistant cancer cells (Zhao et al., 2009). While a possible contributor to the interaction, there was only minor biotransformation of 20(S)-Rh2 into 20(S)-protopanaxadiol in Caco-2 cells in our previous study (Xie et al., 2005). Accordingly, the inhibitory effects on P-gp function we observed should come mainly from 20(S)-Rh2 rather than its metabolite, 20(S)-protopanaxadiol.

Our earlier research showed that 100 μM verapamil and 10 μM cyclosporin A enhanced the accumulation of 20(S)-Rh2 in Caco-2 cells (Xie et al., 2005). We speculated at the time that 20(S)-Rh2 might be a substrate of P-gp. There was also an alternative possibility that 20(S)-Rh2 might be a substrate of other transporters in Caoco-2 cells, which could be inhibited by verapamil and cyclosporin A. In fact, cyclosporin A and verapamil are reported to be inhibitors of BCRP (Ozvegy et al., 2001) and MRPs (Bai et al., 2004). Whether 20(S)-Rh2 is a substrate for these transporters or P-gp was unclear. Accordingly, the transport of 20(S)-Rh2 in Caco-2 cells was investigated further. Unexpectedly, the efflux ratio of 20(S)-Rh2 was found

to be approximately two and was not influenced by 10 μM verapamil, indicating that 20(S)-Rh2 is not a P-gp substrate. In agreement with this finding, Liu *et al*. reported an efflux ratio for 20(S)-Rh2 that was close to one (Liu et al., 2009), which is similar to our results.

Furthermore, we examined the duration of action of 20(S)-Rh2. The third generation P-gp inhibitors XR9576 and GF120918, which were not themselves substrates, exhibited slowly reversible inhibitory effects on P-gp function after removal of the modulator from the incubation medium. In contrast, cyclosporine A and verapamil which were known to be both P-gp inhibitors and substrates lost their inhibitory effects rapidly (Mistry et al., 2001; Pires et al., 2006). The action of 20(S)-Rh2 was different from the classic competitive inhibitor verapamil, but similar to that of XR9576 and GF120918, as the inhibitory effect of 20(S)-Rh2 persisted at least 3 h after removal from the media.

From a pharmacological perspective, noncompetitive inhibitors, such as XR9576, can bind with high affinity to P-gp but are not themselves substrates, which prevent ATP hydrolysis and transport of cytotoxic agent out of the cell, resulting in an increased intracellular concentration (Thomas and Coley, 2003).

In consideration of the protracted duration of inhibitory effect, we tested whether 20(S)-Rh2 affected two key steps of P-gp function: ATPase hydrolysis and P-gp conformation change. Unlike P-gp substrates, 20(S)-Rh2 neither stimulated P-gp ATPase nor increased UIC-2 binding. In fact, 20(S)-Rh2 inhibited P-gp ATPase and decreased UIC-2 binding at high concentrations, unlike what is expected for a P-gp

substrate. Many P-gp substrates, such as verapamil, vinblastine and ritonavir, inhibit the function of P-gp by competing the drug-binding site in P-gp with other P-gp substrates (Dantzig et al., 1996). They stimulate P-gp ATPase and increase UIC-2 binding. With regard to other noncompetitive P-gp inhibitors, sodium orthovanadate, tariquidar (XR9576) and *cis-(Z)*-flupentixol, which are not P-gp substrates, exert their effects on P-gp function *via* allosteric modulation by interacting with other sites in P-gp (Maki et al., 2006). Their actions are completely different from the competitive inhibitors, as indicated by the inhibition of P-gp ATPase hydrolysis and decrease of UIC-2 binding (Maki et al., 2003). Considering all the above, 20(S)-Rh2 may be a noncompetitive inhibitor which interacts with P-gp allosterically by trapping P-gp in a transition-state conformation to inhibit P-gp ATPase without competing for the substrate site.

Since 20(S)-Rh2 was shown to be a potent noncompetitive P-gp inhibitor *in vitro*, we next examined its effects on P-gp function *in vivo*. Specifically, we asked whether 20(S)-Rh2 be used as an intestinal absorption enhancer for P-gp substrate drugs based on a herb-drug interaction. To answer these questions, *in situ* and *in vivo* models were adopted. The ileum, with its high level of P-gp expression, was chosen for an *in situ* intestinal perfusion experiment and an evaluation of the effect of 20(S)-Rh2 on drug absorption. Rhodamine 123 was used as the P-gp substrate probe, given that it had much better water solubility compared to other P-gp substrates of interest. In the presence of 20(S)-Rh2, there was an obvious increase in absorption rate constant and intestinal permeability by nearly 50%, compared to the control

group, which indicated marked inhibition by 20(S)-Rh2 of intestinal P-gp.

To further investigate the interactions of 20(S)-Rh2 with P-gp *in vivo*, pharmacokinetic studies of P-gp substrates after intragastric administration were performed in SD rats with or without coadministration of 20(S)-Rh2. Three P-gp substrates were chosen, among which digoxin and fexofenadine represented prototypical P-gp probes, while etoposide, as a clinical anticancer drug, provided a clinically relevant case example. The oral bioavailability of Rh2 is low (Gu et al., 2009), which is a common characteristic for most botanic origin drugs such as the flavonoid chrysin (Wang and Morris, 2007). Accordingly, a relatively high dose of Rh2 (25 mg/kg; but far below toxic dose in rats) was chosen for our *in vivo* experiment. Results revealed that intragastric administration of 25 mg/kg 20(S)-Rh2 significantly enhanced the AUC and C_{max} of all three P-gp substrates without notable influence on the terminal elimination half-life, which suggested 20(S)-Rh2 increased intestinal absorption but not the systemic elimination of P-gp substrates. This finding was in accordance with our *in situ* results. Similar transporter based absorption enhancement *in vivo* was also found between the flavonoid chrysin and nitrofurantoin (Wang and Morris, 2007).

Herb-drug interactions based on P-gp inhibition are of great clinical concern. Inhibition of P-gp not only can enhance the oral bioavailability of P-gp substrates, including many anti-cancer drugs, but it also reverse multidrug resistance induced by chemotherapeutic agents (Lancet et al., 2009; Kwak et al., 2010). In the present study, 20(S)-Rh2 enhanced the oral bioavailability of etoposide by 4.72-fold, suggesting that

20(S)-Rh2 may have promise as an adjuvant for chemotherapeutic agents based on P-gp inhibition. However, further investigation is needed to determine whether the combination of 20(S)-Rh2 with P-gp substrate drugs can induce some unexpected systemic effect.

Function and protein expression are often tightly linked. Many P-gp inhibitors can strongly induce the expression of P-gp, in addition to the direct inhibitory effect they have on P-gp function (Hou et al., 2008). We tested whether 20(S)-Rh2 could exert a similar dual action effect at the intestinal barrier that protects the body from exposure to toxins. In our experiment, intragastric administration of 20(S)-Rh2 for 10 successive days failed to affect the pharmacokinetic parameters of etoposide 24-hours after the last 20(S)-Rh2 dose, which indirectly indicated that long-term treatment of 20(S)-Rh2 did not alter the expression of P-gp in the intestine. Results from a Western blotting assay directly confirmed that 20(S)-Rh2 did not influence basal P-gp expression in the intestine. Therefore, the effects of 20(S)-Rh2 after long time treatment should be restricted to P-gp inhibition.

In summary, our results suggest that 20(S)-Rh2 is a potent noncompetitive P-gp inhibitor. It can increase the absorption/bioavailability of P-gp substrate drugs including some chemotherapeutic agents when co-administered by the oral route. Moreover, long-term treatment of 20(S)-Rh2 does not affect the intestinal expression of P-gp in rats, indicating that P-gp inhibition should be sustained with multiple dose administration.

DMD Fast Forward. Published on September 13, 2010 as DOI: 10.1124/dmd.110.034793
This article has not been copyedited and formatted. The final version may differ from this version.

ACKNOWLEDGEMENTS

The authors wish to sincerely thank post-graduates Xiaozhou Wen, Ying Zhou, Fang Niu, Yuan Sun and Xuefang Cheng (Key Lab of Drug Metabolism and Pharmacokinetics, China Pharmaceutical University, Nanjing, China) for their assistance.

REFERENCES

Bai J, Lai L, Yeo HC, Goh BC and Tan TM (2004) Multidrug resistance protein 4 (MRP4/ABCC4) mediates efflux of bimane-glutathione. *Int J Biochem Cell Biol* **36:**247-257.

Bardelmeijer HA, Beijnen JH, Brouwer KR, Rosing H, Nooijen WJ, Schellens JH and van Tellingen O (2000) Increased oral bioavailability of paclitaxel by GF120918 in mice through selective modulation of P-glycoprotein. *Clin Cancer Res* **6:**4416-4421.

Chan E, Tan M, Xin J, Sudarsanam S and Johnson DE (2010) Interactions between traditional Chinese medicines and Western therapeutics. *Curr Opin Drug Discov Devel* **13:**50-65.

Chang C, Bahadduri PM, Polli JE, Swaan PW and Ekins S (2006) Rapid identification of P-glycoprotein substrates and inhibitors. *Drug Metab Dispos* **34:**1976-1984.

Dantzig AH, Shepard RL, Cao J, Law KL, Ehlhardt WJ, Baughman TM, Bumol TF and Starling JJ (1996) Reversal of P-glycoprotein-mediated multidrug resistance by a potent cyclopropyldibenzosuberane modulator, LY335979. *Cancer Res* **56:**4171-4179.

Fei XF, Wang BX, Tashiro S, Li TJ, Ma JS and Ikejima T (2002) Apoptotic effects of ginsenoside Rh2 on human malignant melanoma A375-S2 cells. *Acta Pharmacol Sin* **23:**315-322.

Fu LW, Zhang YM, Liang YJ, Yang XP and Pan QC (2002) The multidrug resistance of tumour cells was reversed by tetrandrine in vitro and in xenografts derived

from human breast adenocarcinoma MCF-7/adr cells. *Eur J Cancer* **38:**418-426.

Gu Y, Wang GJ, Sun JG, Jia YW, Wang W, Xu MJ, Lv T, Zheng YT and Sai Y (2009) Pharmacokinetic characterization of ginsenoside Rh2, an anticancer nutrient from ginseng, in rats and dogs. *Food Chem Toxicol* **47:**2257-2268.

Gu Y, Wang GJ, Sun JG, Jia YW, Xie HT and Wang W (2006) Quantitative determination of ginsenoside Rh2 in rat biosamples by liquid chromatography electrospray ionization mass spectrometry. *Anal Bioanal Chem* **386:**2043-2053.

Gu Y, Wang GJ, Wu XL, Zheng YT, Zhang JW, Ai H, Sun JG and Jia YW (2010) Intestinal absorption mechanisms of ginsenoside Rh2: stereoselectivity and involvement of ABC transporters. *Xenobiotica* **doi:10.3109/00498254.2010.500744**.

Hasegawa H, Sung JH, Matsumiya S, Uchiyama M, Inouye Y, Kasai R and Yamasaki K (1995) Reversal of daunomycin and vinblastine resistance in multidrug-resistant P388 leukemia in vitro through enhanced cytotoxicity by triterpenoids. *Planta Med* **61:**409-413.

Hou XL, Takahashi K, Tanaka K, Tougou K, Qiu F, Komatsu K and Azuma J (2008) Curcuma drugs and curcumin regulate the expression and function of P-gp in Caco-2 cells in completely opposite ways. *Int J Pharm* **358:**224-229.

Jia WW, Bu X, Philips D, Yan H, Liu G, Chen X, Bush JA and Li G (2004) Rh2, a compound extracted from ginseng, hypersensitizes multidrug-resistant tumor

cells to chemotherapy. *Can J Physiol Pharmacol* **82:**431-437.

Kikuchi Y, Sasa H, Kita T, Hirata J, Tode T and Nagata I (1991) Inhibition of human ovarian cancer cell proliferation in vitro by ginsenoside Rh2 and adjuvant effects to cisplatin in vivo. *Anticancer Drugs* **2:**63-67.

Kim HS, Lee EH, Ko SR, Choi KJ, Park JH and Im DS (2004) Effects of ginsenosides Rg3 and Rh2 on the proliferation of prostate cancer cells. *Arch Pharm Res* **27:**429-435.

Kitagawa I, Yoshikawa M, Yoshihara M, Hayashi T and Taniyama T (1983) [Chemical studies of crude drugs (1). Constituents of Ginseng radix rubra]. *Yakugaku Zasshi* **103:**612-622.

Kwak JO, Lee SH, Lee GS, Kim MS, Ahn YG, Lee JH, Kim SW, Kim KH and Lee MG (2010) Selective inhibition of MDR1 (ABCB1) by HM30181 increases oral bioavailability and therapeutic efficacy of paclitaxel. *Eur J Pharmacol* **627:**92-98.

Lancet JE, Baer MR, Duran GE, List AF, Fielding R, Marcelletti JF, Multani PS and Sikic BI (2009) A phase I trial of continuous infusion of the multidrug resistance inhibitor zosuquidar with daunorubicin and cytarabine in acute myeloid leukemia. *Leuk Res* **33:**1055-1061.

Liu H, Yang J, Du F, Gao X, Ma X, Huang Y, Xu F, Niu W, Wang F, Mao Y, Sun Y, Lu T, Liu C, Zhang B and Li C (2009) Absorption and disposition of ginsenosides after oral administration of Panax notoginseng extract to rats. *Drug Metab Dispos* **37:**2290-2298.

Maki N, Hafkemeyer P and Dey S (2003) Allosteric modulation of human P-glycoprotein. Inhibition of transport by preventing substrate translocation and dissociation. *J Biol Chem* **278:**18132-18139.

Maki N, Moitra K, Ghosh P and Dey S (2006) Allosteric modulation bypasses the requirement for ATP hydrolysis in regenerating low affinity transition state conformation of human P-glycoprotein. *J Biol Chem* **281:**10769-10777.

Marchetti S, Mazzanti R, Beijnen JH and Schellens JH (2007) Concise review: Clinical relevance of drug drug and herb drug interactions mediated by the ABC transporter ABCB1 (MDR1, P-glycoprotein). *Oncologist* **12:**927-941.

Mechetner EB, Schott B, Morse BS, Stein WD, Druley T, Davis KA, Tsuruo T and Roninson IB (1997) P-glycoprotein function involves conformational transitions detectable by differential immunoreactivity. *Proc Natl Acad Sci U S A* **94:**12908-12913.

Mistry P, Stewart AJ, Dangerfield W, Okiji S, Liddle C, Bootle D, Plumb JA, Templeton D and Charlton P (2001) In vitro and in vivo reversal of P-glycoprotein-mediated multidrug resistance by a novel potent modulator, XR9576. *Cancer Res* **61:**749-758.

Nishimura T, Kato Y, Amano N, Ono M, Kubo Y, Kimura Y, Fujita H and Tsuji A (2008) Species difference in intestinal absorption mechanism of etoposide and digoxin between cynomolgus monkey and rat. *Pharm Res* **25:**2467-2476.

Ozvegy C, Litman T, Szakacs G, Nagy Z, Bates S, Varadi A and Sarkadi B (2001) Functional characterization of the human multidrug transporter, ABCG2,

expressed in insect cells. *Biochem Biophys Res Commun* **285:**111-117.

Petri N, Tannergren C, Rungstad D and Lennernas H (2004) Transport characteristics of fexofenadine in the Caco-2 cell model. *Pharm Res* **21:**1398-1404.

Pires MM, Hrycyna CA and Chmielewski J (2006) Bivalent probes of the human multidrug transporter P-glycoprotein. *Biochemistry* **45:**11695-11702.

Qiu J (2007) 'Back to the future' for Chinese herbal medicines. *Nat Rev Drug Discov* **6:**506-507.

Rengelshausen J, Banfield M, Riedel KD, Burhenne J, Weiss J, Thomsen T, Walter-Sack I, Haefeli WE and Mikus G (2005) Opposite effects of short-term and long-term St John's wort intake on voriconazole pharmacokinetics. *Clin Pharmacol Ther* **78:**25-33.

Sun M, Xu X, Lu Q, Pan Q and Hu X (2007) Schisandrin B: a dual inhibitor of P-glycoprotein and multidrug resistance-associated protein 1. *Cancer Lett* **246:**300-307.

Takeuchi T, Yoshitomi S, Higuchi T, Ikemoto K, Niwa S, Ebihara T, Katoh M, Yokoi T and Asahi S (2006) Establishment and characterization of the transformants stably-expressing MDR1 derived from various animal species in LLC-PK1. *Pharm Res* **23:**1460-1472.

Thomas H and Coley HM (2003) Overcoming multidrug resistance in cancer: an update on the clinical strategy of inhibiting p-glycoprotein. *Cancer Control* **10:**159-165.

Ujie K, Oda M, Kobayashi M and Saitoh H (2008) Relative contribution of absorptive

and secretory transporters to the intestinal absorption of fexofenadine in rats. *Int J Pharm* **361:**7-11.

Wang X and Morris ME (2007) Effects of the flavonoid chrysin on nitrofurantoin pharmacokinetics in rats: potential involvement of ABCG2. *Drug Metab Dispos* **35:**268-274.

Wang Z, Zheng Q, Liu K, Li G and Zheng R (2006) Ginsenoside Rh(2) enhances antitumour activity and decreases genotoxic effect of cyclophosphamide. *Basic Clin Pharmacol Toxicol* **98:**411-415.

Xie HT, Wang GJ, Chen M, Jiang XL, Li H, Lv H, Huang CR, Wang R and Roberts M (2005) Uptake and metabolism of ginsenoside Rh2 and its aglycon protopanaxadiol by Caco-2 cells. *Biol Pharm Bull* **28:**383-386.

Xie X, Eberding A, Madera C, Fazli L, Jia W, Goldenberg L, Gleave M and Guns ES (2006) Rh2 synergistically enhances paclitaxel or mitoxantrone in prostate cancer models. *J Urol* **175:**1926-1931.

Xu WL, Shen HL, Ao ZF, Chen BA, Xia W, Gao F and Zhang YN (2006) Combination of tetrandrine as a potential-reversing agent with daunorubicin, etoposide and cytarabine for the treatment of refractory and relapsed acute myelogenous leukemia. *Leuk Res* **30:**407-413.

Zhao Y, Bu L, Yan H and Jia W (2009) 20S-protopanaxadiol inhibits P-glycoprotein in multidrug resistant cancer cells. *Planta Med* **75:**1124-1128.

FOOTNOTE

J.Z. and F.Z. contributed equally to this work.

This work was supported by China National Nature Science Foundation (No.30973583 and No.30801411); China 'Creation of New Drugs' Key Technology Projects (No. 2009ZX09304-001 and 2009ZX09502-004); Jiangsu Province Nature Science Foundation (No. BK2008038).

Figures and legends

Fig 1 Structure of 20(S)-Rh2.

Fig 2 Effects of 20(S)-Rh2 on the accumulation of rhodamine 123 in Caco-2 cells. Cells were preincubated with 20(S)-Rh2 for 1.5 h followed by a further 2 h incubation in the presence of 5 μM rhodamine. Data are the mean ± S.E. of three independent experiments. $^{**}p<0.01$ *vs* control

Fig 3 Effects of 20(S)-Rh2 on the transport of P-gp substrates across Caco-2 monolayers. Cells were preincubated for 1.5 h in the presence of 20(S)-Rh2 and followed by co-incubation for 2 h in the presence of 5 μM digoxin (A) or 10 μM fexofenadine (B) or 10 μM etoposide (C). Data are the mean ± S.E. of three independent experiments. $^{*}p<0.05$ *vs* control; $^{**}p<0.01$ *vs* control

Fig 4 Transport characteristics of 20(S)-Rh2 across Caco-2 cell monolayers. 20(S)-Rh2 (1, 5, 10 μM) was loaded on either AP or BL side and incubated for 1.5 h. Digoxin was used as positive P-gp substrate control. Verapamil was used as positive P-gp inhibitor control. Data are the mean ± S.E. of three independent experiments.

Fig 5 Duration of P-gp inhibitory effect of 20(S)-Rh2. Caco-2 cells were exposed to 10 μM 20(S)-Rh2 for 1.5 h, washed, and incubated in 20(S)-Rh2 free medium for the indicated periods prior to the addition of 5 μM rhodamine 123 and further incubation for 2 h. T_0 represents the end of the 20(S)-Rh2 incubation phase. Verapamil was used

as positive control. Data are the mean ± S.E. of three independent experiments. $^{**}p<0.01$ *vs* T_0.

Fig 6 Effects of 20(S)-Rh2 on basal and verapamil-stimulated ATPase activity of P-gp. Human P-gp-overexpressing membranes obtained from baculovirus-infected insect cells were incubated with indicated concentrations of 20(S)-Rh2 in the absence (A) or presence (B) of 20 μM verapamil. Data are the mean ± S.E. of three independent experiments. $^{*}p<0.05$ *vs* control; $^{**}p<0.01$ *vs* control; $^{\#}p<0.05$ *vs* verapamil 20 μM; $^{\#\#}p<0.01$ *vs* verapamil 20 μM.

Fig 7 Effects of 20(S)-Rh2 on the binding of conformation-sensitive antibody UIC2 to P-gp. (A) Effects of 1 μM and 10 μM 20(S)-Rh2, 10 μM vinblastine (normal substrate control), 1 mM Na_3VO_4 (ATPase inhibitor control) on UIC2 binding were studied. Cells incubated with normal IgG_{2a} were included as a background control, and DMSO treatment was used as a solvent control. (B) Results quantified from three independent experiments are presented as mean ± S.E. $^{**}p<0.01$ *vs* control

Fig 8 Plasma concentration-time curves in semi-log scale of digoxin (A), fexofenadine (B) or etoposide (C) in control and 20(S)-Rh2 pre-treated male SD rats. The smaller figures represent the data in normal scale. The control groups were given intragastrically a dose of 0.25 mg/kg digoxin, 10 mg/kg fexofenadine or 10 mg/kg etoposide, respectively. The pre-treated groups were intragastrically administered a dose of 25 mg/kg 20(S)-Rh2, 2 h prior to digoxin, fexofenadine or

etoposide dose. Data are expressed as mean ± S.E., n = 5 per group.

Fig 9 Plasma concentration-time curves of etoposide in control and 20(S)-Rh2 long-term-treated male SD rats. The control group were given blank vehicle for 10 successive days, and the long-term-treated groups were intragastrically administered a dose of 25 mg/kg 20(S)-Rh2 for 10 successive days. On the 11^{th} day, a dose of 10 mg/kg etoposide was given intragastrically to both groups. Data are expressed as mean ± S.E., n = 5 per group.

Fig 10 Effects of 20(S)-Rh2 on P-gp expression levels in Caco-2 cells and in rat ileum. (A) Caco-2 cells were exposed to 1 μM , 10 μM 20(S)-Rh2 or vehicle for 24, 48, and 72 h. (B) Expression of P-gp protein in the ileum of rats administered intragastrically vehicle or 20(S)-Rh2 at a dose of 25 mg/kg for 10 successive days. Rats were sacrificed on day 11. The upper is the representative blots. The lower is the bar graph that shows the quantification of band intensity. Data are expressed as mean ± S.E.

Tables

Table 1 Analytical conditions in LC-MS/MS analysis

Compound	Ionization Mode	m/z	Mobile Phase A	Mobile Phase B	Gradient Condition (B concentration%)
Digoxin	ESI (-)	779.4→649.2	0.02% aqueous ammonia	acetonitrile	0min;20%→0.5min;20%→1min;65%→3min;
Digitoxin (IS)		763.5→633.2 (IS)			65%→4.5min; 20%→7min;20%
Fexofenadine	ESI (+)	502.4→466.2	0.1% formic acid	acetonitrile	0min;18% → 1min;18% → 4min;90% →
Loratadine (IS)		383.4→337.1 (IS)			6min;90%→6.3min;18%→10min;18%
Etoposide	ESI (+)	606.2→229.0	0.1% formic acid + 2mM	acetonitrile	0min;15%- → 0.8min;15% → 3min;85% →
Fexofenadine (IS)		502.4→466.2 (IS)	ammonium formate		5min;85%→5.5min;20%→9min;15%

DMD Fast Forward. Published on September 13, 2010 as DOI: 10.1124/dmd.110.034793
This article has not been copyedited and formatted. The final version may differ from this version.

Table 2 Effects of 20(S)-Rh2 on absorption rate constant k_a and permeability of rhodamine 123 in the single-pass intestinal perfusion model in rats

	Absorption rate constant, k_a ($\times 10^{-3}$ min^{-1})	Intestinal permeability ($\times 10^{-5}$ cm sec^{-1})
Control (1% ethanol)	33.4 ± 1.2	4.4 ± 0.2
20(S)-Rh2 1 μM	42.3 ± 0.6 **	6.0 ± 0.1 **
20(S)-Rh2 5 μM	54.7 ± 2.0 **	8.0 ± 0.5 **
20(S)-Rh2 10 μM	58.3 ± 3.6 **	8.0 ± 0.2 **
Verapamil 50 μM	64.4 ± 3.5 **	9.6 ± 0.6 **

P_{eff} and k_a values are presented as mean ± S.E; Studies were conducted in triplicate in each experimental group

** $p<0.01$, *vs* control.

Fig 1

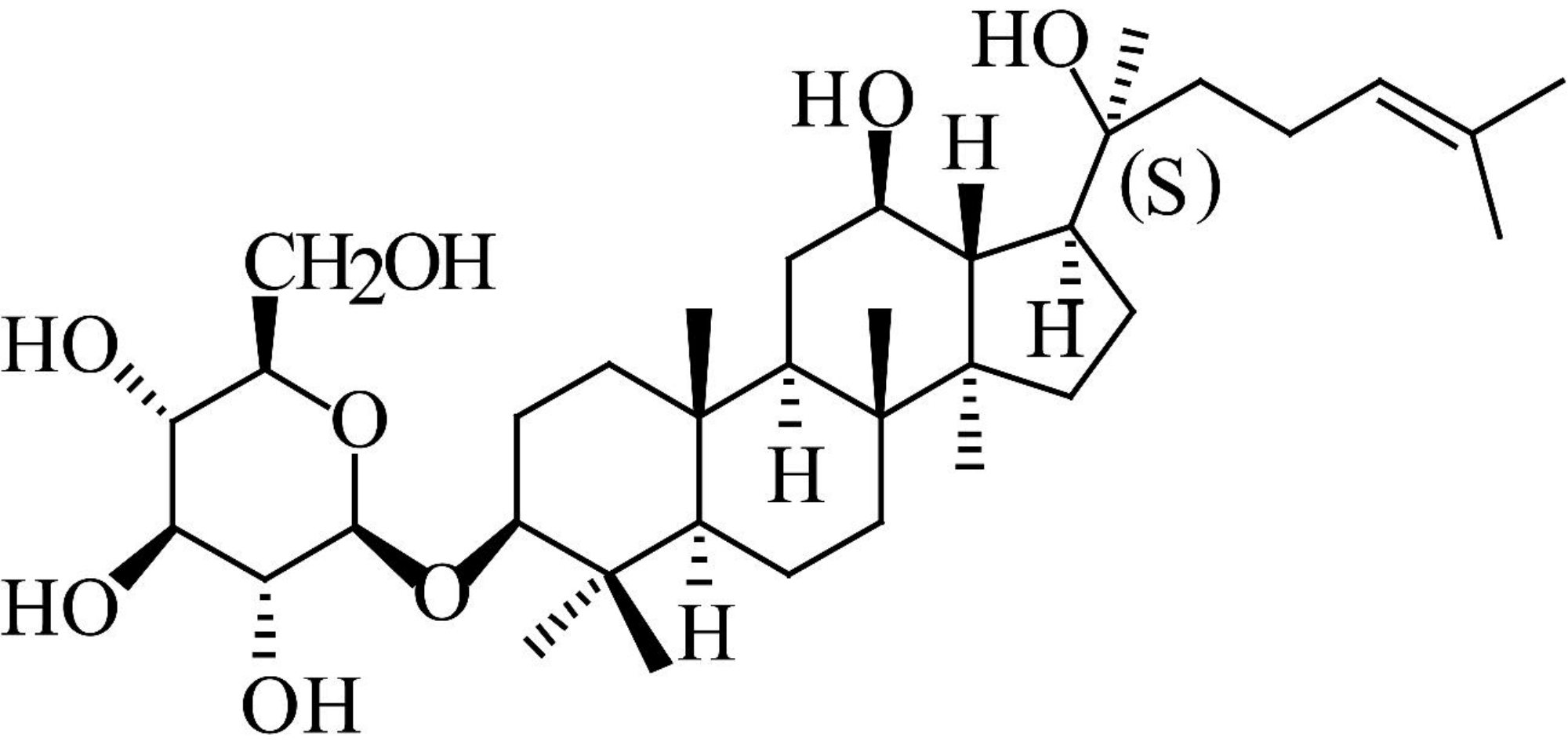

Fig 2

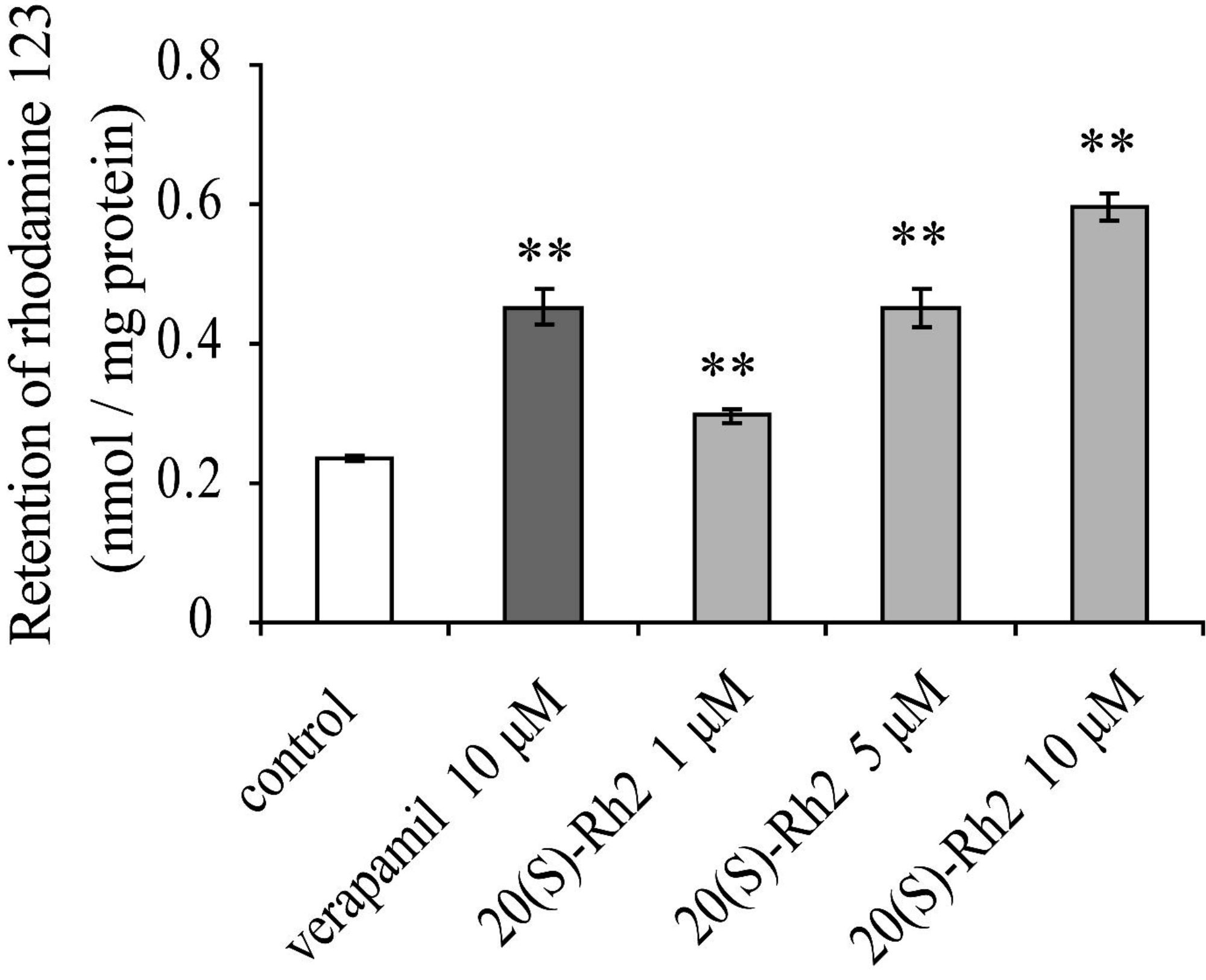
Retention of rhodamine 123
(nmol / mg protein)
0.8
0.6
0.4
0.2
0
**
**
**
**
control
verapamil 10 μM
20(S)-Rh2 1 μM
20(S)-Rh2 5 μM
20(S)-Rh2 10 μM

Fig 3

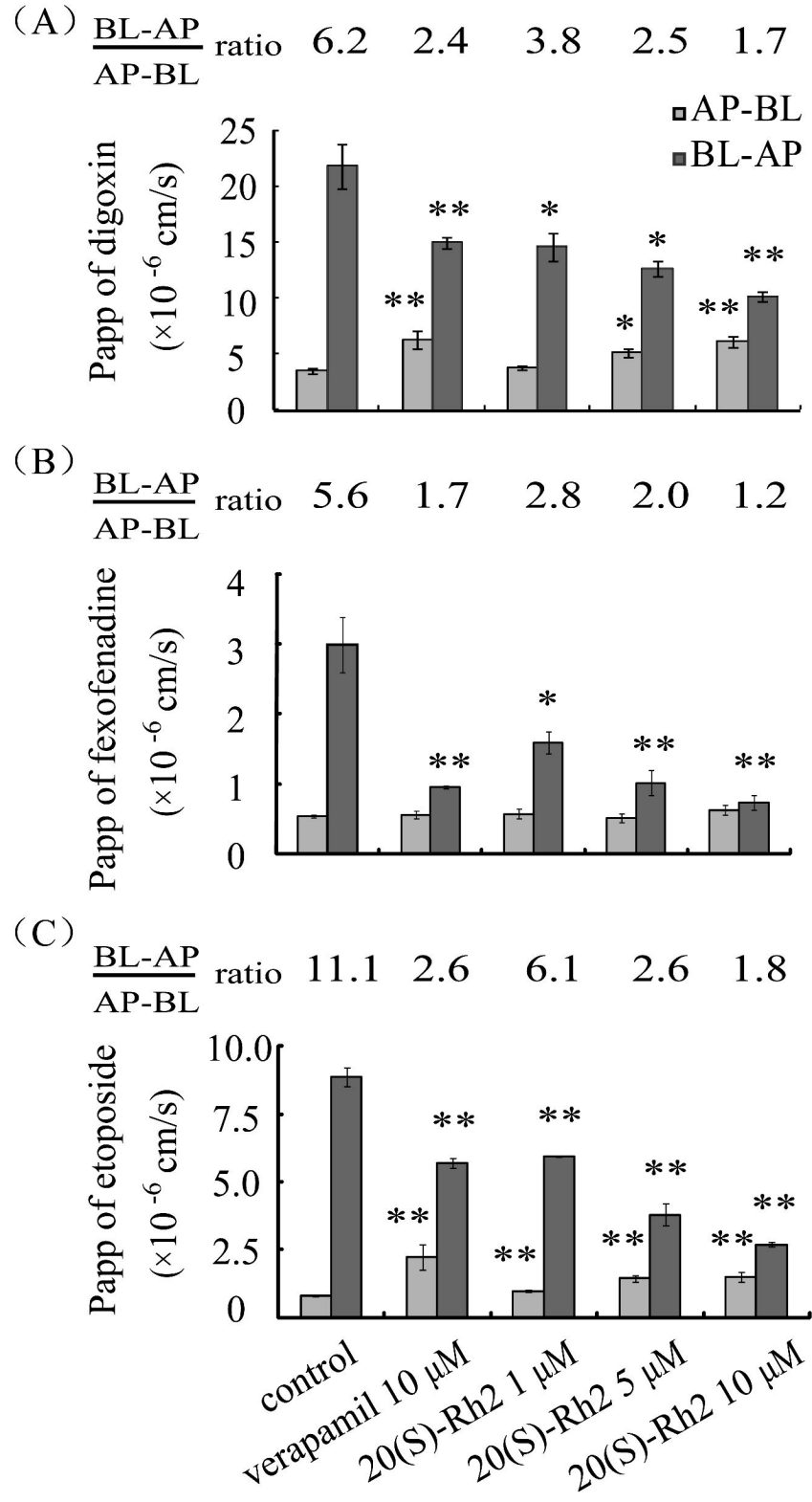
(A)
BL-AP / AP-BL ratio 6.2 2.4 3.8 2.5 1.7
AP-BL
BL-AP
Papp of digoxin (×10 -6 cm/s)
25
20
15
10
5
0
(B)
BL-AP / AP-BL ratio 5.6 1.7 2.8 2.0 1.2
Papp of fexofenadine (×10 -6 cm/s)
4
3
2
1
0
(C)
BL-AP / AP-BL ratio 11.1 2.6 6.1 2.6 1.8
Papp of etoposide (×10 -6 cm/s)
10.0
7.5
5.0
2.5
0
control
verapamil 10 μM
20(S)-Rh2 1 μM
20(S)-Rh2 5 μM
20(S)-Rh2 10 μM

Fig 4

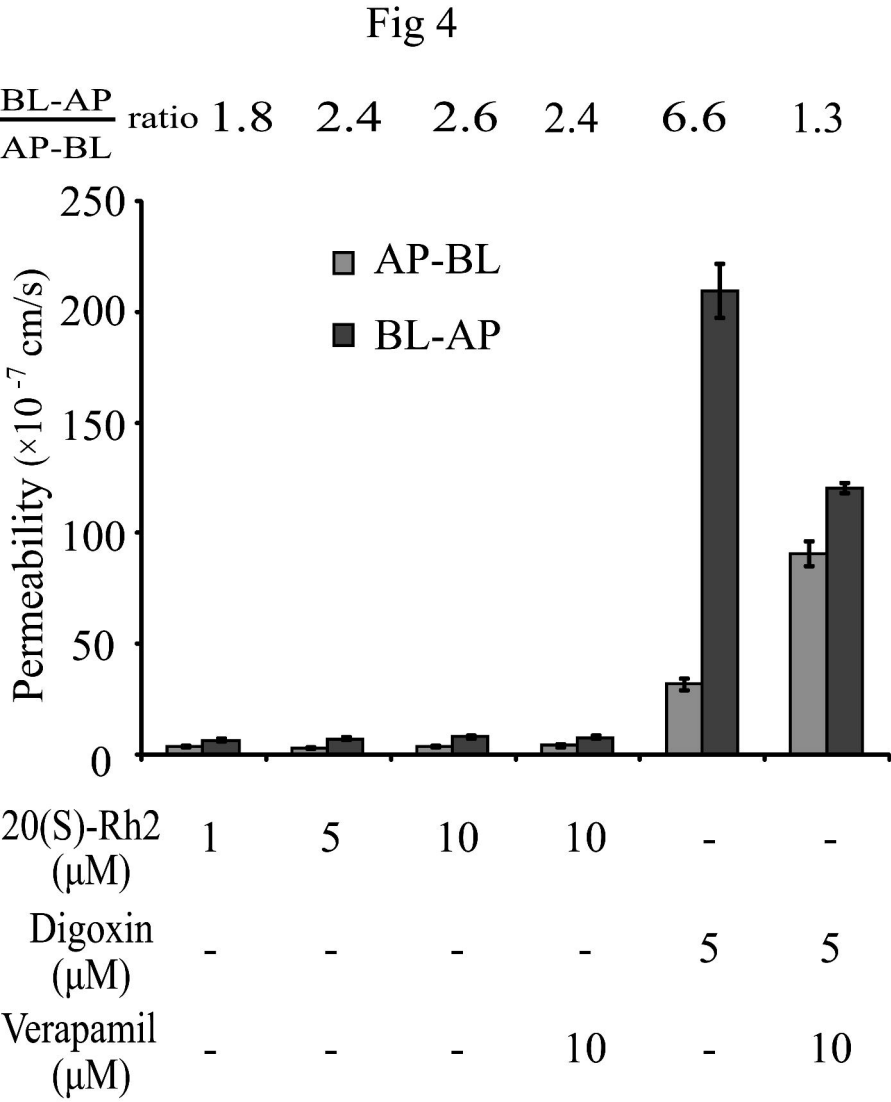
BL-AP / AP-BL ratio
1.8
2.4
2.6
2.4
6.6
1.3
250
200
150
100
50
0
Permeability (×10 -7 cm/s)
AP-BL
BL-AP
20(S)-Rh2 (μM)
1
5
10
10
-
-
Digoxin (μM)
-
-
-
-
5
5
Verapamil (μM)
-
-
-
10
-
10

Fig 5

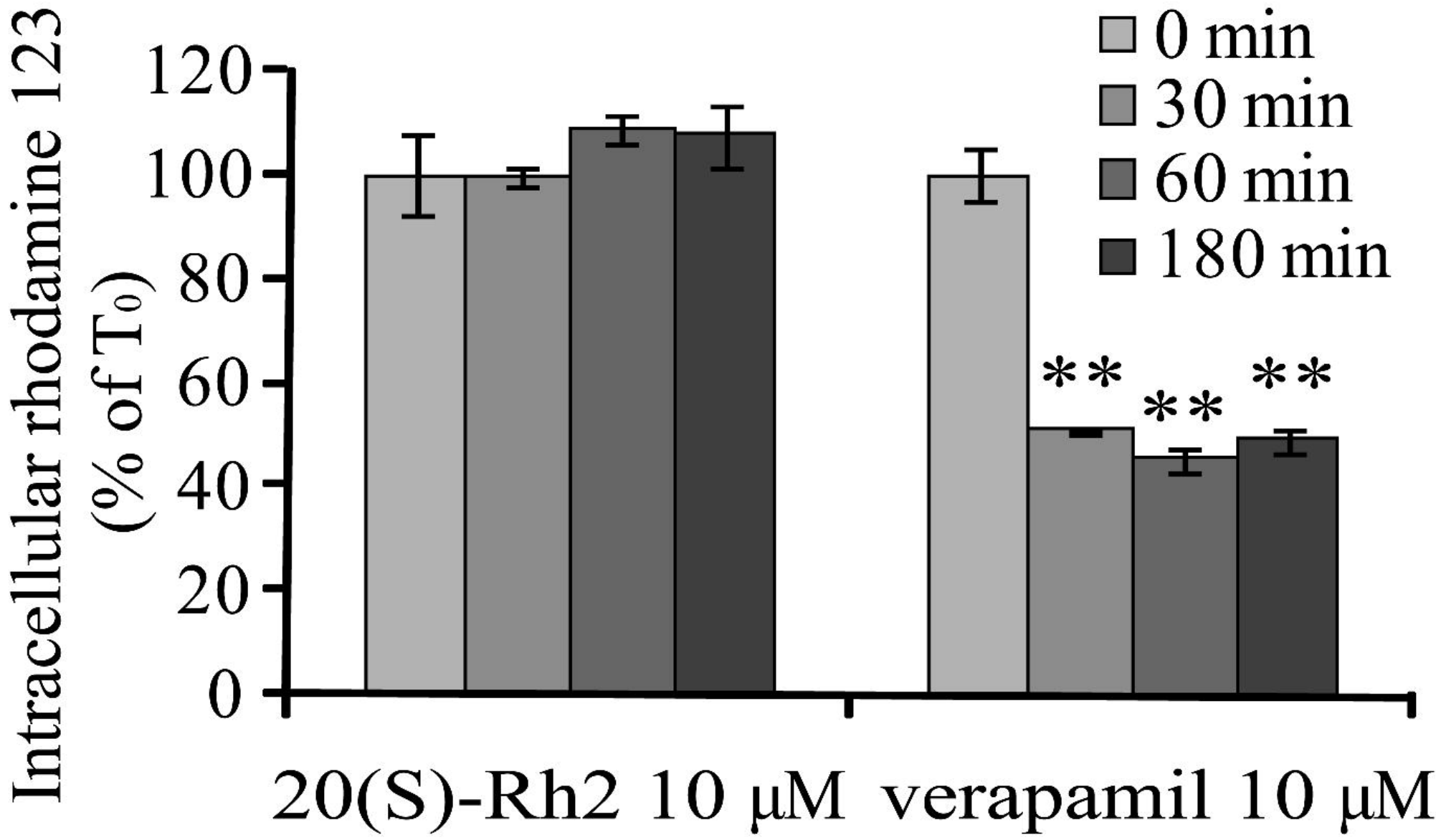
Intracellular rhodamine 123
(% of T0)
120
100
80
60
40
20
0
0 min
30 min
60 min
180 min
**
**
**
20(S)-Rh2 10 μM
verapamil 10 μM

Fig 6

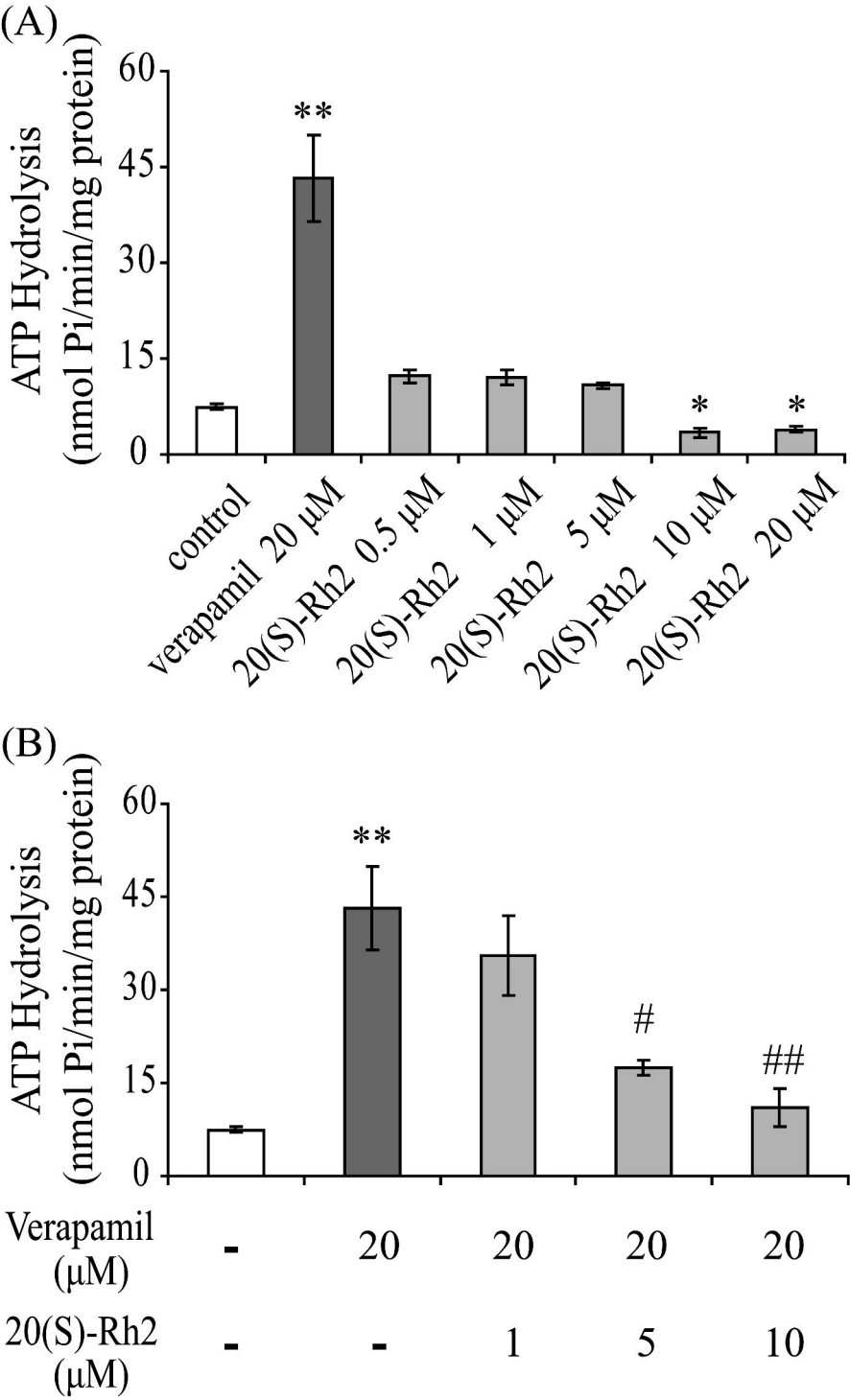
(A)
ATP Hydrolysis
(nmol Pi/min/mg protein)
60
45
30
15
0
**
*
*
control
verapamil 20 μM
20(S)-Rh2 0.5 μM
20(S)-Rh2 1 μM
20(S)-Rh2 5 μM
20(S)-Rh2 10 μM
20(S)-Rh2 20 μM
(B)
ATP Hydrolysis
(nmol Pi/min/mg protein)
60
45
30
15
0
**
#
##
Verapamil (μM)
- 20 20 20 20
20(S)-Rh2 (μM)
- - 1 5 10

Fig 7

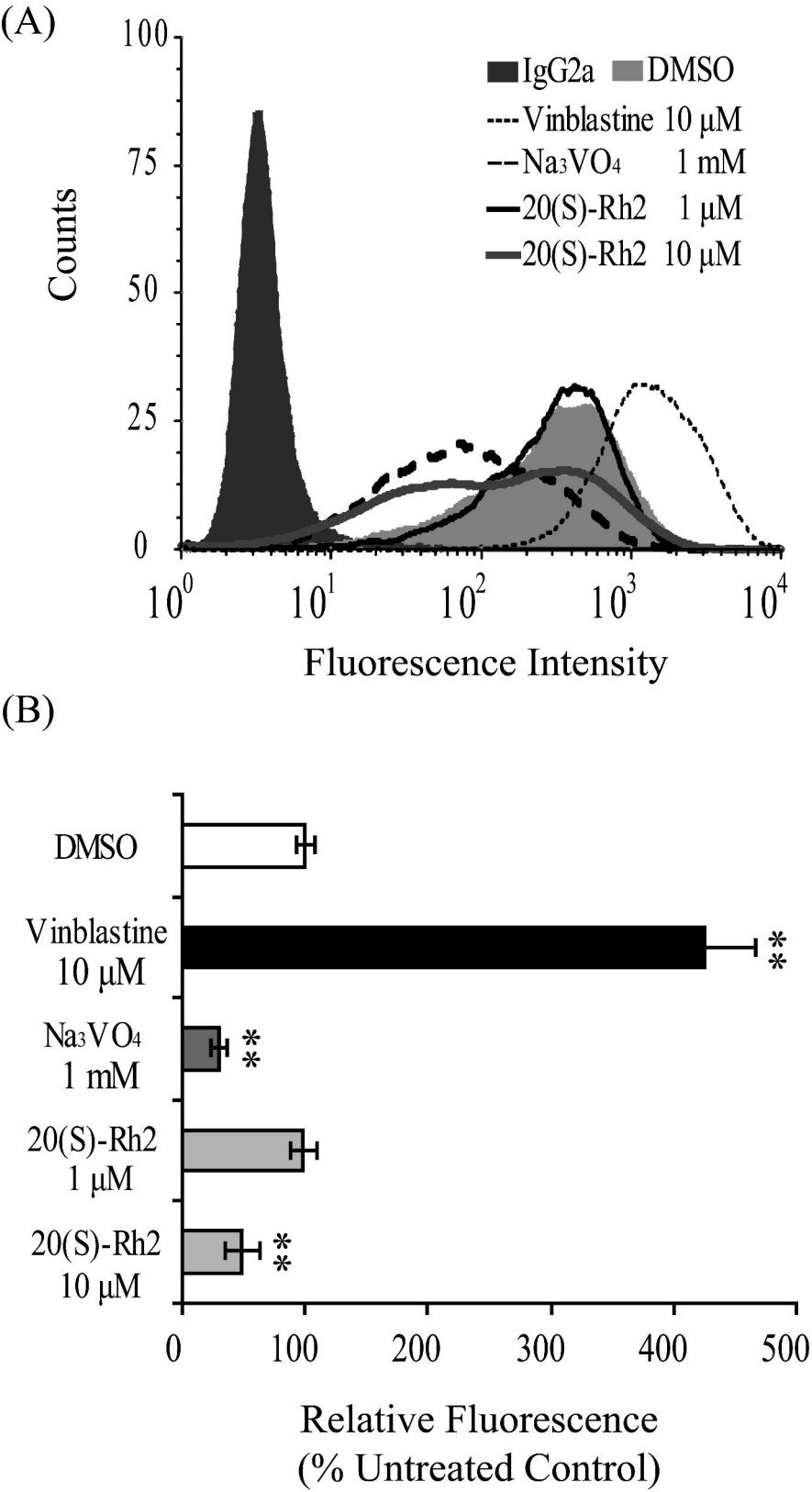
(A)
100
75
50
25
0
Counts
IgG2a
DMSO
Vinblastine 10 μM
Na3VO4 1 mM
20(S)-Rh2 1 μM
20(S)-Rh2 10 μM
10^0
10^1
10^2
10^3
10^4
Fluorescence Intensity
(B)
DMSO
Vinblastine 10 μM
Na3VO4 1 mM
20(S)-Rh2 1 μM
20(S)-Rh2 10 μM
**
**
**
0
100
200
300
400
500
Relative Fluorescence
(% Untreated Control)

Fig 8

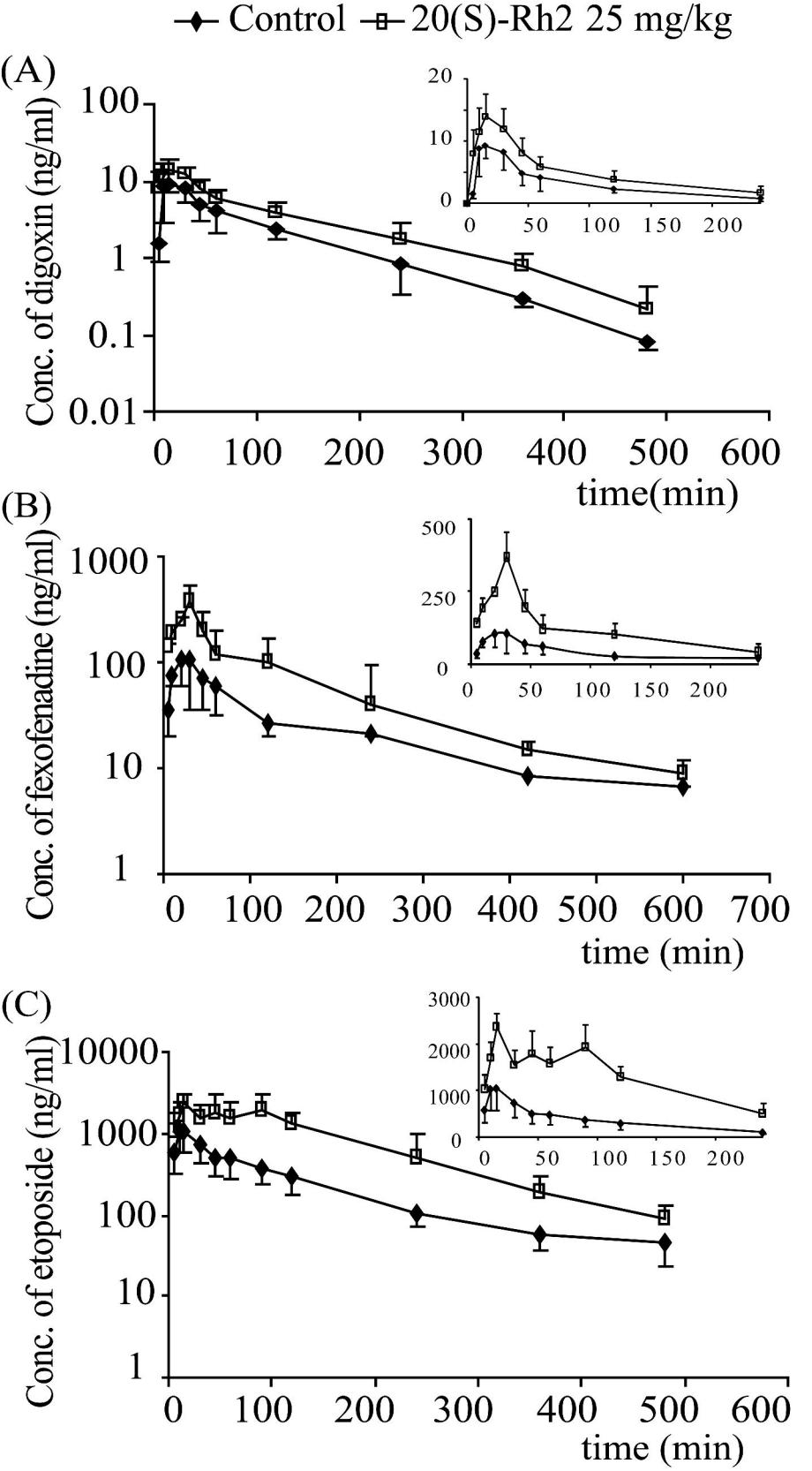
Control
20(S)-Rh2 25 mg/kg
(A)
Conc. of digoxin (ng/ml)
100
10
1
0.1
0.01
0
100
200
300
400
500
600
time(min)
20
10
0
0
50
100
150
200
(B)
Conc. of fexofenadine (ng/ml)
1000
100
10
1
0
100
200
300
400
500
600
700
time (min)
500
250
0
0
50
100
150
200
(C)
Conc. of etoposide (ng/ml)
10000
1000
100
10
1
0
100
200
300
400
500
600
time (min)
3000
2000
1000
0
0
50
100
150
200

Fig 9

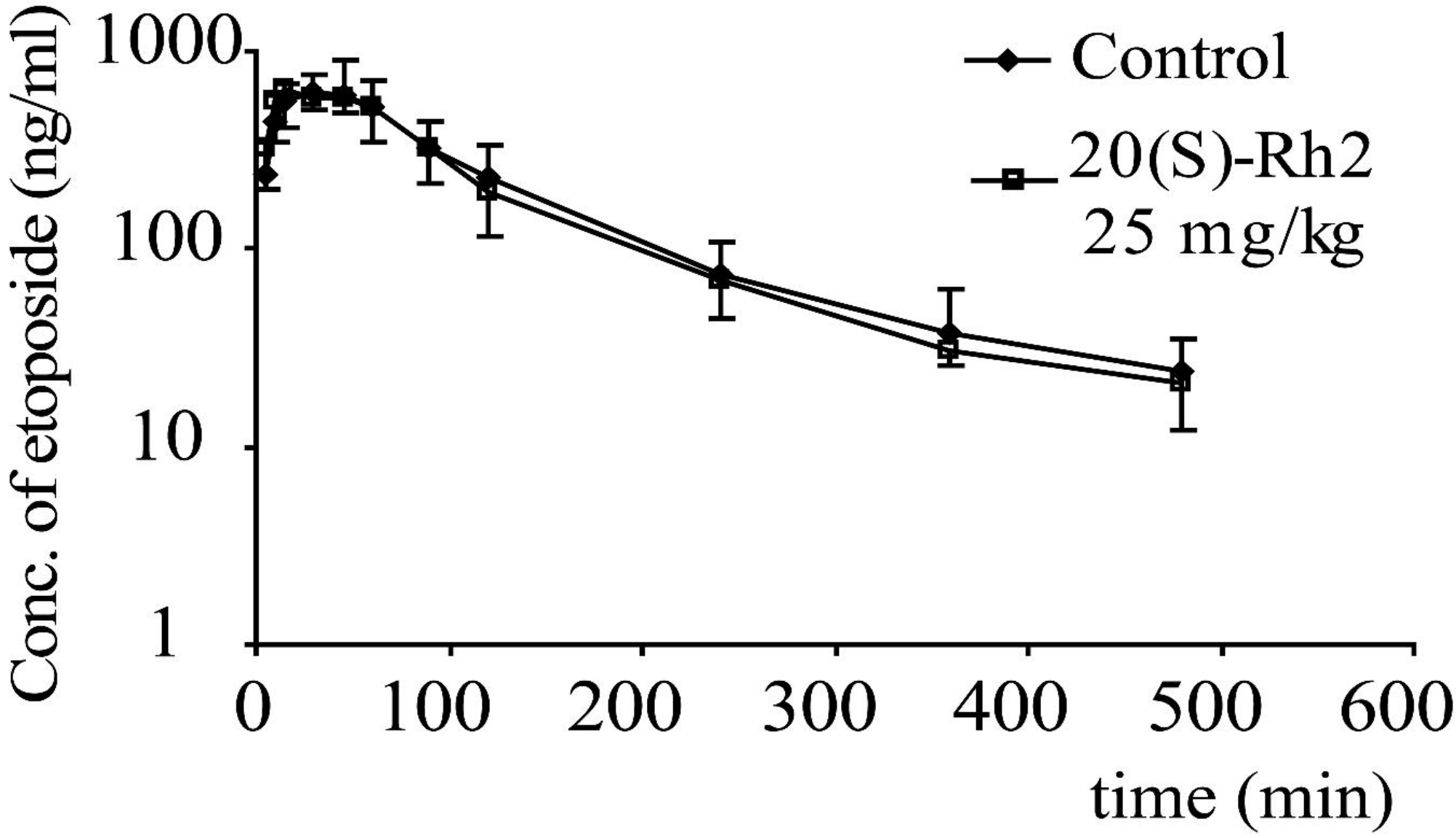
Conc. of etoposide (ng/ml)
1000
100
10
1
0
100
200
300
400
500
600
time (min)
Control
20(S)-Rh2
25 mg/kg

Fig 10

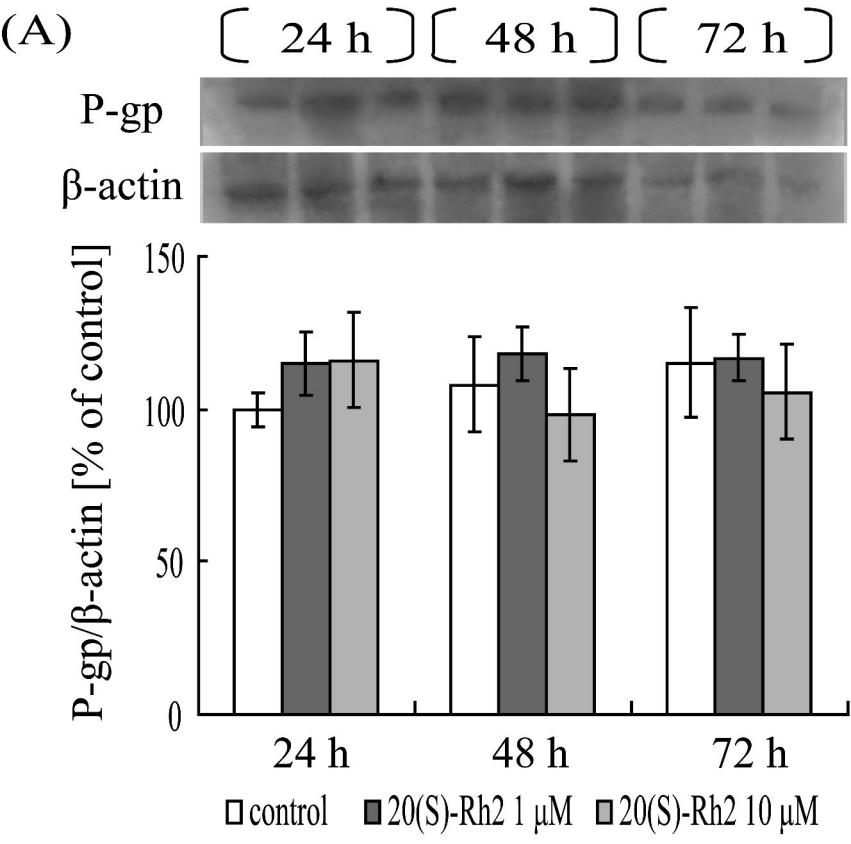
(A)
24 h
48 h
72 h
P-gp
β-actin
P-gp/β-actin [% of control]
150
100
50
0
24 h
48 h
72 h
control
20(S)-Rh2 1 μM
20(S)-Rh2 10 μM

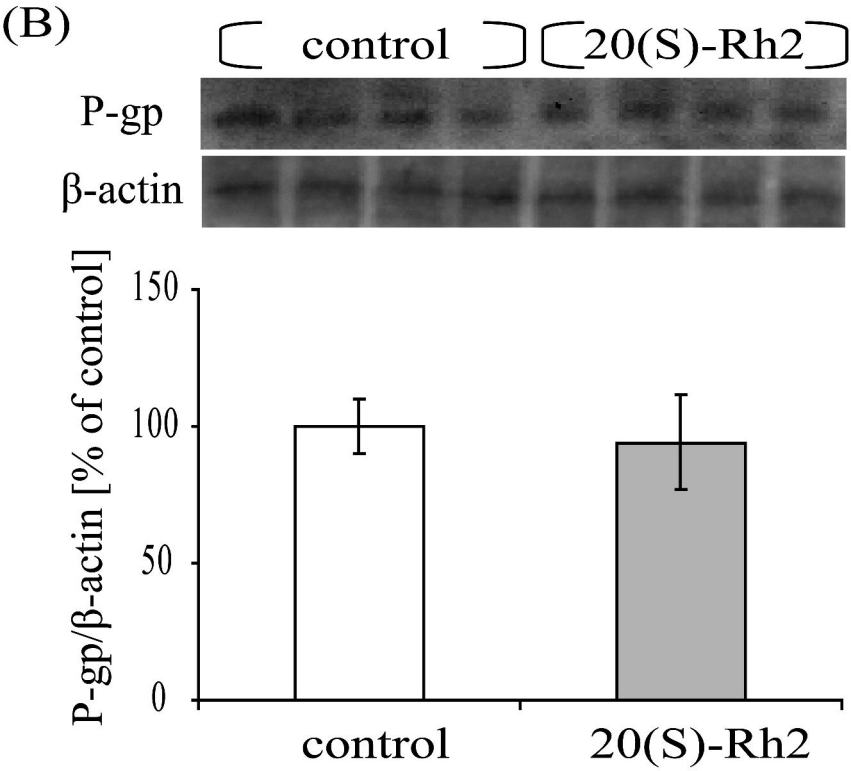
(B)
control
20(S)-Rh2
P-gp
β-actin
P-gp/β-actin [% of control]
150
100
50
0
control
20(S)-Rh2